NONLINEAR VIBRATION OF A THREE-DIMENSIONAL MOVING GANTRY CRANE SUBJECTED TO A TRAVELLING TROLLEY HOISTING A SWINGING OBJECT

Davood Younesian[1], Elyas Ghafoori[2], Mehdi Sadeghpour[3]
[1] *School of Railway Engineering, Iran University of Science and Technology, Narmak, Tehran, 16846, Iran*
[2] *School of Mechanical Engineering, Swiss Federal Institute of Technology Lausanne, Lausanne, Switzerland*
[3] *Mechanical Engineering Department, Sharif University of Technology, Tehran, Iran*
E-mail: younesian@iust.ac.ir

Received February 2009, Accepted July 2010
No. 09-CSME-05, E.I.C. Accession 3091

ABSTRACT

Nonlinear vibration of a three-dimensional moving gantry crane carrying a trolley hoisting a swinging object is studied in this paper. A finite element method is used to solve nonlinear coupled governing equations of the structure. A combinational technique (Newmark-Runge-Kutta) is employed for direct integration procedure. To develop a comprehensive parametric study and sensitivity analysis of the coupled nonlinear system, sequence of numerical simulations are carried out. Parametric study is directed to find out how different parameters like speed and acceleration of the trolley and gantry crane as well as the mass of the moving trolley and swinging object may affect the linear and nonlinear responses of the structure. It is found that the nonlinearity arises from large amplitude of three-dimensional motion of the swinging object.

Keywords: Nonlinear vibration; gantry crane; swinging object; finite element method.

VIBRATION NON LINÉAIRE D'UNE GRUE À PORTIQUE TRIDIMENSIONNELLE EN MOUVEMENT ASSUJETTIE À UN CHARIOT DÉPLAÇANT UN OBJET OSCILLANT

RÉSUMÉ

Le sujet de l'article est la vibration non linéaire d'une grue à portique tridimensionnelle en mouvement portant un chariot déplaçant un objet oscillant. Nous utilisons une méthode d'éléments finis pour résoudre les équations non linéaires couplées régissant les équations de la structure. Une technique combinée (Newmark-Runge-Kutta) est employée pour le processus d'intégration directe. Pour élaborer une étude paramétrique approfondie et l'analyse de la sensibilité du système non linéaire couplé, des séquences de simulations sont effectuées. Des investigations paramétriques ont aussi été réalisées afin de savoir comment les différents paramètres comme la vitesse et l'accélération du chariot et de la grue portique ainsi que la masse de chariot en mouvement et de l'objet oscillant peuvent affecter les réponses linéaires et non linéaires de la structure. Les résultats démontrent que la non linéarité se produit à cause de l'amplitude du mouvement oscillatoire de l'objet.

Mots-clés: Vibration non linéaire; grue à portique; objet oscillant; méthode d'éléments finis.

1. INTRODUCTION

Dynamic analysis of structures subjected to moving object(s) as a very important and practical engineering problem has received a lot of interests during last decade. Vibration of bridges, gantry cranes, railway tracks and missile launchers are some examples in this regard. Many researchers have conducted different studies in this field. Fryba [1] has presented some fundamentals in this area and also cited more than 200 references in this field included most of the published research done before 1999. Most of the papers in this area neglect the effects of moving mass inertia and the moving object is assumed to act as a moving force [2]. There are even fewer studies that take into account the inertia effects due to the mass of the moving objects [3]. Lee [4] studied the dynamic response of a beam due to a moving mass and showed that separation of the mass from the beam may occur for a relatively slow speed and small mass when the beam is clamped at both ends. Lin [5] and Esmailzadeh and Ghorashi [6,7] have studied the forced vibration responses of a beam traversed by uniformly and partially distributed moving masses. Xu et al. [8] have investigated a none-linear moving mass problem using finite difference method and perturbation technique. Younesian et al. studied vibration of beams traversed by 6 DOF moving objects [9]. Vibration of infinite beams on visco-elastic foundations has also received notable of interest because of its application in design of railway tracks. Vibration of Timoshenko beams rested on linear, nonlinear and random viscoelastic foundations has been studied by Kargarnovin and Younesian [10–12]. Ghafoori and Asgahri [13] investigated the dynamic response of horizontal and inclined non-isotropic plates under a moving mass using a first-order shear deformation theory (FSDT) and an adaptive finite element method approach. They studied the effect of parameters such as mass and speed of the moving object, the slope of the inclined plate, the ply-angle orientation of the laminate and moving force simplification on the dynamic response of composite plates. They showed that the simplification of the moving mass problem with a moving force one, does not always lead to good results especially for the case of laminated plates. They then presented the laminate stacking orders that result to negligible/substantial difference between the dynamic responses of the moving mass system and its corresponding moving force simplification. Sorensen et al. [14] introduced a control approach to allow accurate positioning of a crane payload, as movement and disturbance-induced oscillations are removed. They also considered several approaches for determining stability of the system. Ghafoori and Ghahremani [15] introduced a semi-analytical method to calculate the dynamic responses of a rectangular plate due to a moving oscillator. The assumed the elastic distributed structure as a general plate (two-dimensional elastic distributed structure). Then they used a combination of the Fourier and Laplace transformation as well as the convolution theorem to solve the governing differential equations and finally a modified integration technique has been presented to solve the coupled governing differential equations of motion. Singhose et al. [16] used the command generation method of input shaping to decrease the residual vibration of a planar gantry crane with hoisting of the load. A comprehensive literature survey shows that vibration of beam-type structures has received considerable attention, but there are very few investigations in the area of vibration of frames subjected to moving objects. Most of the papers focused on transverse vibration of beams, however, in the case of vibration of frames, transverse, lateral and longitudinal vibrations of beam-columns should be taken into consideration. A three-dimensional vibration ($\overline{X}$, $\overline{Y}$ and $\overline{Z}$) of a space frame structure due to a two-dimensional moving mass has been investigated by Wu [17]. Wu also used FEM and studied the dynamic response of a three-dimensional framework subjected to moving carriage hoisting a swinging object using the equivalent moving mass matrix [18].

The main objective of the present paper is to analyze the vibration of mobile gantry cranes that are commonly used in industrial plants, rail-head freight yards and ports all over the world. Gantry crane are equipped with wheels and move along a parallel pair of rails in the ($\bar{y}$) direction as shown in Fig. 1. As it is illustrated in Fig. 2, for simplicity the moving trolley and swinging object are modeled, respectively, with a moving lumped mass (m_t) and a swinging lumped object (m_{SO}). Inertia effects of all the moving objects are taken into account. In addition, it is assumed that the gantry crane, moving trolley, and swinging object all have velocity and acceleration. In this paper nonlinear vibration of a three-dimensional moving gantry crane carrying a trolley hoisting a swinging object is studied. Nonlinearity arises from large amplitude of three-dimensional motion of the swinging object. It should be noted that reaching large amplitudes is quite probable in practice and linearization of the equations of motion may induce a major errors in simulation. Finite element formulation is presented in section 2. Solution procedure is then presented in section 3, and numerical simulations and parametric study are discussed in section 4. This paper is an extended version of a conference paper presented in 7th EUROMECH Solid Mechanics Conference held at Portugal [19].

2. FINITE ELEMENT FORMULATION

Equation of motion for multiple degree of freedom structure is given by

$$[\bar{M}]\{\ddot{q}\} + [\bar{C}]\{\dot{q}\} + [\bar{K}]\{q\} = \{\bar{F}(t)\} \tag{1}$$

where $[\bar{M}]$, $[\bar{C}]$ and $[\bar{K}]$ are overall mass, damping, and stiffness matrices, respectively. Moreover, $\{\bar{F}(t)\}$ is the external force vector, and $\{\ddot{q}\}$, $\{\dot{q}\}$ and $\{q\}$ are the acceleration, velocity, and displacement vectors, respectively.

The stiffness and mass matrices as well as the damping matrix are explained in appendices A and B.

As it is seen in Fig. 1, θ represents the angle of swinging object in x-y plane and ϕ denotes the angle between swinging object and x-y plane. Also in Fig. 3, f_x, f_y, f_z are the three components

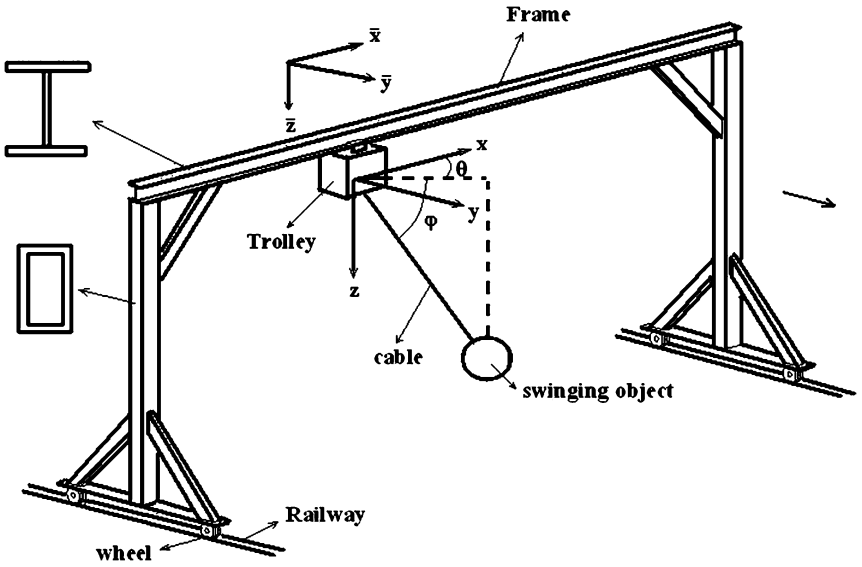

Fig. 1. Tree-dimensional sketch of the mobile gantry crane.

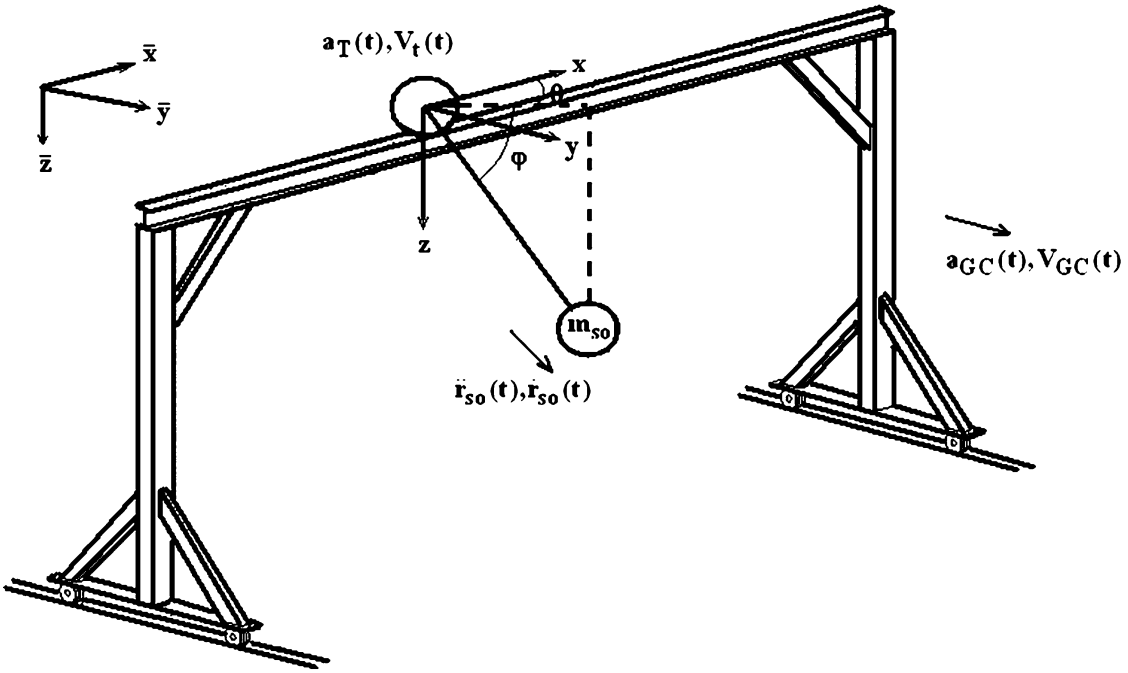

Fig. 2. Generalized coordinates of the 3D motion.

of the external force vector which is created between the moving moving trolley and the frame, in other words, the effect of the system of the trolley and the swinging object is considered by this virtual external force vector. Figure 4 shows the swinging object position with respect to the local coordinate system. It can be seen that

$$\begin{cases} x = r\cos\phi\cos\theta \\ y = r\cos\phi\sin\theta \\ z = r\sin\phi \end{cases} \tag{2}$$

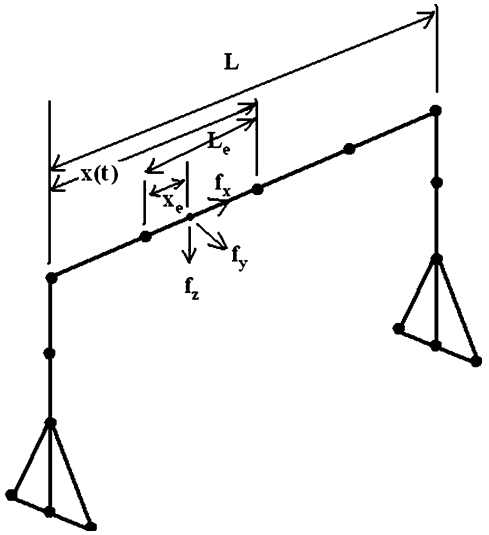

Fig. 3. Finite element model of gantry crane.

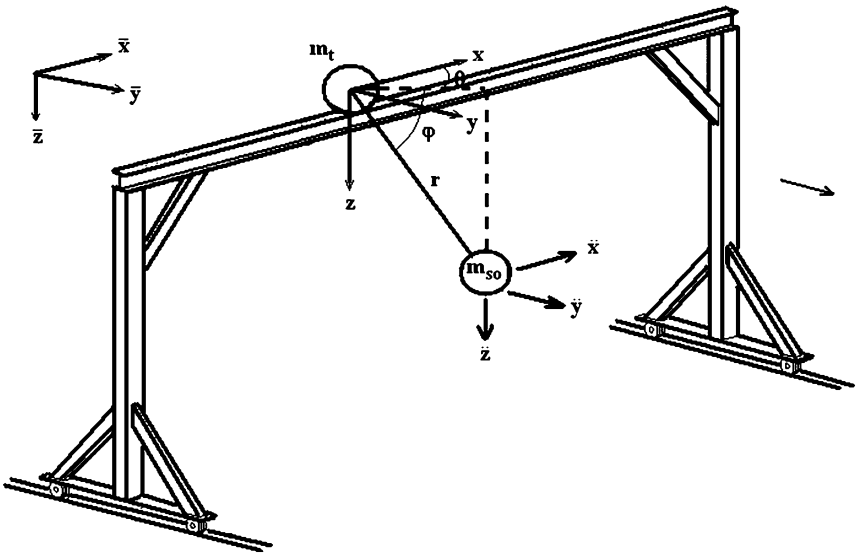

Fig. 4. Position and acceleration of the swinging object with respect to the local coordinate system.

where x, y, z are the position components of the swinging object with respect to the local coordinate system.

From Fig. 5 and Newton's equations of motion for swinging mass, it can be concluded that

$$\begin{cases} -F\cos\phi\cos\theta = m_{SO}(\ddot{x}+\ddot{u}+a_T) \\ -F\cos\phi sin\theta = m_{SO}(\ddot{y}+\ddot{v}+a_{GC}) \\ -F\sin\phi + m_{SO}g = m_{SO}(\ddot{z}+\ddot{w}) \end{cases} \tag{3}$$

where F is the cable tension, a_T is the acceleration of the trolley in the x direction and a_{GC} is the acceleration of the gantry crane in the y direction. Also, m_t is the moving lumped mass and m_{SO}

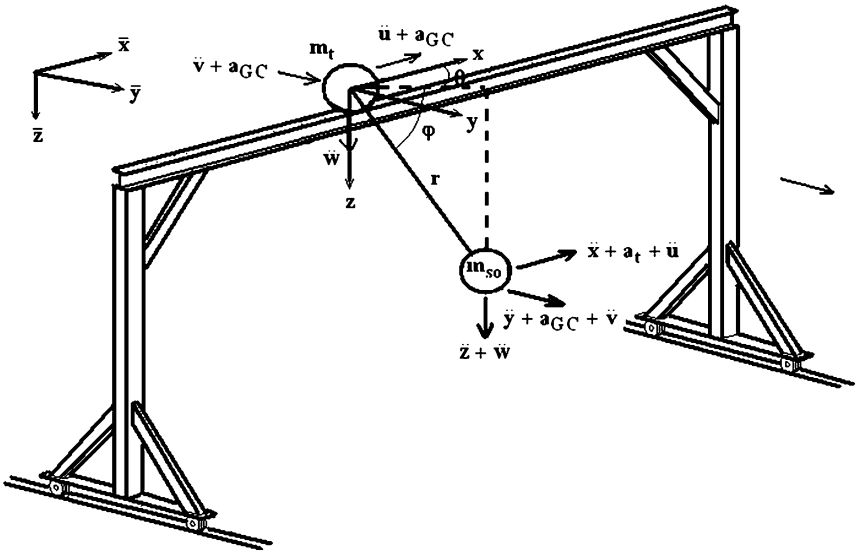

Fig. 5. Acceleration of trolley and swinging object with respect to the global coordinate system.

is the swinging lumped object. $\ddot{u}$,$\ddot{v}$ *and* $\ddot{w}$ are the translational acceleration of the local coordinate system (xyz).

From Eq. (2), $\ddot{x}$,$\ddot{y}$ *and* $\ddot{z}$- the components of the acceleration of the swinging object with respect to the local coordinate system - can be obtained ($\ddot{x}$, $\ddot{y}$ *and* $\ddot{z}$ is given in the appendix C).

From Fig. 5 and Newton's equations of motion for trolley, it can be seen that

$$\begin{cases} F\cos\phi\cos\theta = m_T(\ddot{u}+a_T)+f_x \\ F\cos\phi\sin\theta = m_T(\ddot{v}+a_{GC})+f_y \\ F\sin\phi + m_T g = m_T\ddot{w}+f_z \end{cases} \tag{4}$$

Also, from Eq. (3) it is obvious that

$$\begin{cases} \tan\theta = \dfrac{\ddot{y}+\ddot{v}+a_{GC}}{\ddot{x}+\ddot{u}+a_T} \\ g + \dfrac{(\ddot{x}+\ddot{u}+a_T)\sin\phi}{\cos\phi\cos\theta} = \ddot{z}+\ddot{w} \end{cases} \tag{5}$$

Substituting Eq. (4) in Eq. (3) yields

$$\begin{cases} f_x = m_T(\ddot{u}+a_T)+m_{SO}(\ddot{x}+\ddot{u}+a_T) \\ f_y = m_T(\ddot{v}+a_{GC})+m_{SO}(\ddot{y}+\ddot{v}+a_{GC}) \\ f_z = m_T\ddot{w}+m_{SO}(\ddot{z}+\ddot{w}) \end{cases} \tag{6}$$

To calculate the value of f_x, f_y *and* f_z, the parameters θ, $\dot{\theta}$, $\ddot{\theta}$, φ, $\dot{\varphi}$ *and* $\ddot{\varphi}$ should be determined. A combinational technique is used for solution of the coupled nonlinear equations of motion. a_{GC} is also the acceleration of the moving Gantry crane and is given in Table 2. The Runge-Kutta technique to solve nonlinear set of Eqs. (5) and the Newmark integration method to solve the Eq. (1) are employed to iterate the response in each time step. In other words, in any time step of the Newmark iteration, one iteration of Runge-Kutta should be performed. Finally, the overall external force vector can be obtained.

3. PROCEDURE OF SOLUTION

The dynamic response of the gantry crane due to moving swinging object may be obtained with the following steps:

1. Use appendix A to find the transformed stiffness $[\bar{k}]$ and mass $[\bar{m}]$ matrices for each element of the structure. Assemble the global stiffness $[\bar{K}]$ and global mass $[\bar{M}]$ matrices using the transformed stiffness $[\bar{k}]$ and mass $[\bar{m}]$ matrices.
2. Determine the overall damping matrix $[\bar{C}]$ using Jacobi method of the theory of Rayleigh damping [20] and the Eqs. (B.1–B.4) in appendix B. It is noted that we should use the overall stiffness $[\bar{K}]$ and mass $[\bar{M}]$ matrices to find the overall damping matrix $[\bar{C}]$. In this study, a damping ratio ξ of 0.03 has been used for the simulated results.
3. Find the global external force vector $\{\bar{F}(t)\}$ at time (t) by using Runge-Kutta technique to solve the nonlinear coupled Eqs. (5). b) Determine the dynamic responses of the gantry crane framework by solving the Eq. (1) using Newmark direct integration method [20].

4. Repeat steps 1–3 with time step Δt=0.01 and for T_{total} which is the time that trolley travels on top beam, it is noted that in step 3, part (a) and part (b) should be run simultaneously.

4. NUMERICAL RESULTS AND DISCUSSION

The structures investigated in this paper are made of steel with mass density of $\rho = 7820\ kg/m^3$ and Young's modulus of $E = 2.06 \times 10^{11}\ N/m^2$. The gravitational acceleration is $g = 9.81\ m/s^2$ and the time step Δt is assumed to be $0.01\ s$.

The gantry crane investigated is made of three major beams: the top beam with a length $L = 12\ m$, the left and the right-side beams with a height of $H = 6m$. The cross sections of the beams are shown in Fig. 6, where for the top beam the cross section of area is $A = 53.8 \times 10^{-4}\ m^2$ and for the left and the right-side beams $A = 32.2 \times 10^{-4}\ m^2$ [18]. The cable used has an initial length and constant acceleration of $l_i = 5m$ and $\dot{l}_i = -5$ cm/s , respectively. Moreover, the mass of the trolley is 10 kg.

4.1. TWO-DIMENSIONAL PORTAL FRAME

In order to verify the solution method presented in this paper, the vibration of the central point of the top beam is obtained, as shown in Fig. 7. Thirty elements are used to simulate the top horizontal beam and twenty elements for each of right and left beams where the vertical beams are clamped at both ends. In this simulation, the moving mass starts its motion from the left hand side of the top beam with a constant velocity of $V = 9\ m/s$, then stops at the middle of the top beam. The influence of the magnitude of the moving mass on the vertical displacements of the central point C_P of the frame ($\bar{Z}_C$) is shown in Fig. 8. In this figure, the solid line (—), the solid line with circle ($-o-$) and the solid line with cross($-+-$) denote, the vertical displacements of the central point C_P due to the moving masses (considering inertial effects of the load) respectively for the magnitudes of m = 500, 300 and 100 kg , whereas the dotted lines (.....) denote to the corresponding static responses for each mass.

From this figure, one can see that the vibration of the middle point is damped while the trolley is stopped at the centre of the top beam and the dynamic response of the central point converges to the static value of the central point deflection. It is reasonable because of the damping effect of the structure.

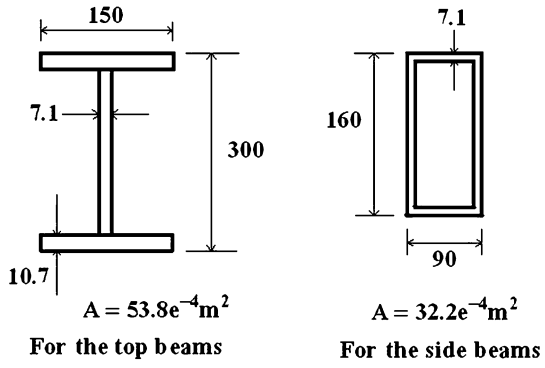

Fig. 6. Cross sections of the beams (dimensions in mm).

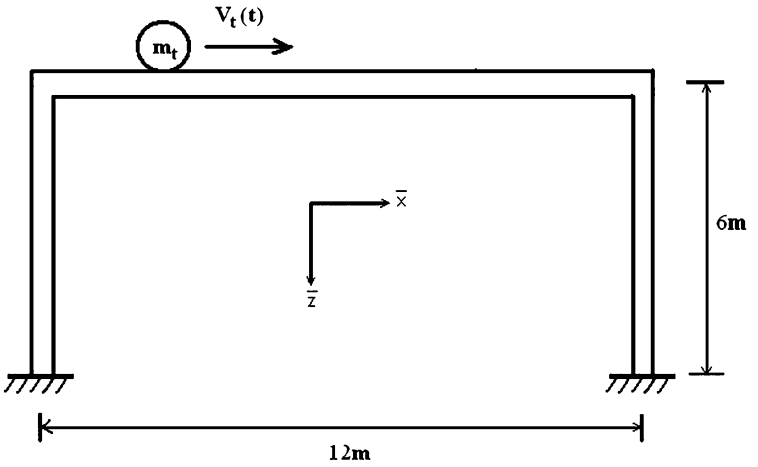

Fig. 7. Two-dimensional stationary gantry crane subjected to a moving mass.

In Fig. 9, the influence of moving-mass speed on the dynamic responses of the frame (the vertical displacements of C_P), is illustrated. There are three different velocity histories for the moving mass that are described in Fig. 10 and Table 1. From Fig. 9, it can be found that the maximum vertical displacement of the central point C_P is equal for the three velocity histories but its profile becomes wider for larger accelerations.

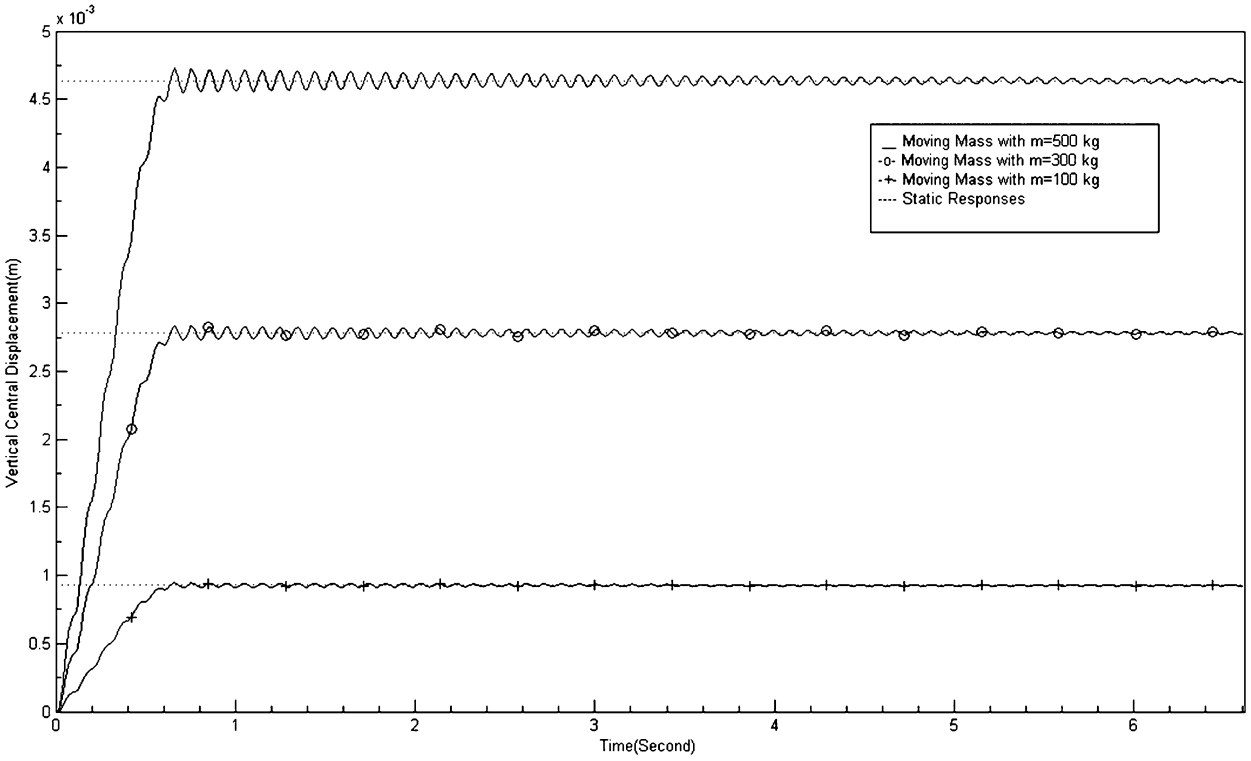

Fig. 8. The influence of magnitude of mass of the trolley on the vertical displacements of the central point C_P.

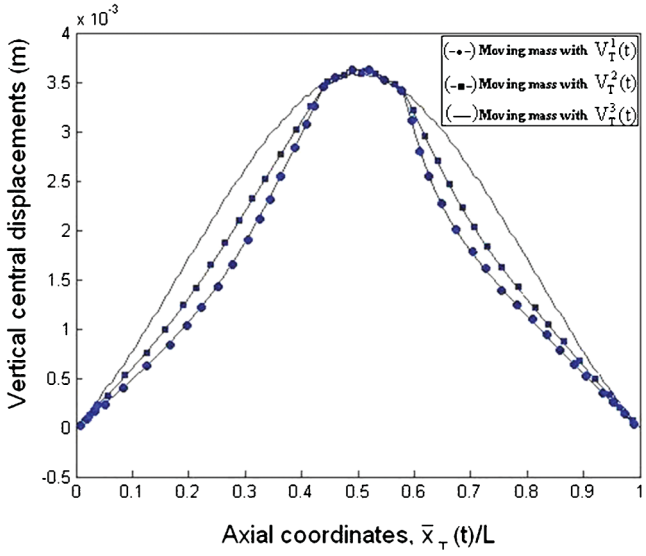

Fig. 9. The influence of moving mass speed on the dynamic responses of the frame C_P.

4.2. Influence of moving mass hoisting a swinging object on two-dimensional portal frame

In this section, dynamic response of a two-dimensional stationary framework as shown in Fig. 11 is studied when it is traversed by a moving trolley hoisting a swinging object. Motion of the swinging object and moving mass are in x-z plane.

Figure 12 shows the influence of the increase of the mass of the swinging object on the vertical displacements of the central point CP. The moving trolley starts its motion from the left hand side of the top beam and stops in the middle of the beam. From this figure it can be seen that the dynamic responses converge to a displacement which is greater than corresponding static response. This is a result of inertia forces of the swinging mass motion.

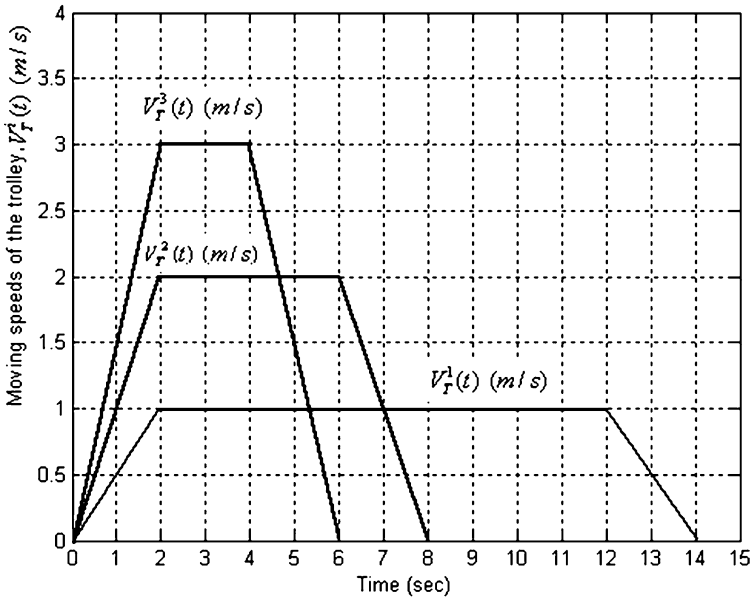

Fig. 10. Three different velocity profiles for the moving mass.

Table 1. Time histories for moving speeds of the trolley; $V_T{}^1(t)$, $V_T{}^2(t)$ and $V_T{}^3(t)$.

(a) Time history of the moving trolley, $V_T^1(t)$						
Time t(s)	0	→	2	12	→	14
$x_T^1(t)$ (m)	0	$\rightarrow^+$	1	11	→	12
$V_T^1(t)$ (m/s)	0	Accelerating	1	1	Decelerating	0
$a_T^1(t)$ $\left(m/s^2\right)$	—	+0.5 *	0	0	–0.5	0
(b) Time history of the moving trolley, $V_T^2(t)$						
Time t(s)	0	→	2	6	→	8
$x_T^2(t)$ (m)	0	→	2	10	→	12
$V_T^2(t)$ (m/s)	0	Accelerating	2	2	Decelerating	0
$a_T^2(t)$ $\left(m/s^2\right)$	—	+1.0	0	0	−1.0	0
(c) Time history of the moving trolley, $V_T^3(t)$						
Time t(s)	0	→	2	4	→	6
$x_T^3(t)$ (m)	0	→	3	9	→	12
$V_T^3(t)$ (m/s)	0	Accelerating	3	3	Decelerating	0
$a_T^3(t)$ $\left(m/s^2\right)$	—	+1.5	0	0	−1.5	0

+. → denotes moving.
*. + denotes acceleration and – denotes deceleration.

Figure 13 illustrates the vertical central vibration of the top beam with a mass of $m_{SO}=400\,kg$ and a moving trolley speed of $V_T^1(t)$ for 45 seconds. Figure 14 depicts the time history of the swinging angle $\theta(t)$ for 50 seconds. It is interesting that the amplitude of the vibration of the swinging angle increases significantly when the trolley stops at the right hand end, and then gradually attenuated to zero. Even more interestingly, the frequency of swinging angle increases as the time passes because of the shortening of the cable length.

Figure 15 illustrates the influence of the speed of the trolley on $\theta(t)$. This figure shows both linear and nonlinear responses of the $\theta(t)$. The mass of the swinging object is $m_{SO}=400$ kg. From this figure it can be seen that the vibration amplitude of the swinging object increases significantly with the increase of acceleration and speed of the trolley.

Table 2. Time history of the velocity of the moving Gantry crane, $V_{GC}(t)$.

Time t(s)	0	→	4	8	→	12
$y_{GC}(t)$ (m)	0	$\rightarrow^+$	2.4	7.2	→	9.6
$V_{GC}(t)$ (m/s)	0	Accelerating	1.2	1.2	Decelerating	0
$a_{GC}(t)$ $\left(m/s^2\right)$	—	+0.3*	0	0	−0.3	0

+. → denotes moving.
*. + denotes acceleration and – denotes deceleration.

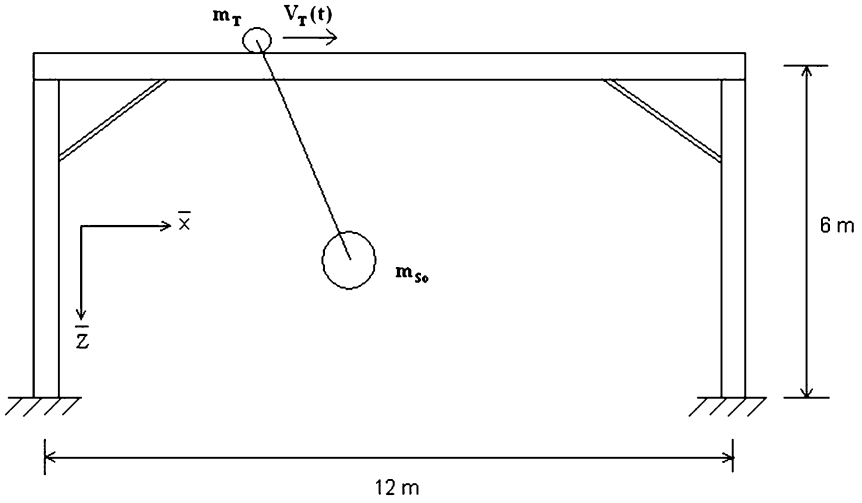

Fig. 11. Two-dimensional stationary gantry crane subjected to a moving trolley hoisting a swinging object.

Moreover, it is noteworthy that when the trolley is stopped suddenly at the right hand end of the portal frame the vibration amplitude of the swinging object increases significantly and then is gradually damped to zero.

Comparing the linear and nonlinear solution, it is interesting to note that the linear solution has the same vibration amplitude as the nonlinear solution; however the nonlinear solution has a time lag with respect to the linear solution. It is also worth noting that for $\theta \leq 6^\circ$ there is no significant difference between the linear and nonlinear solutions; however with the increase of the swinging angle the linear curve gradually diverges from the nonlinear curve.

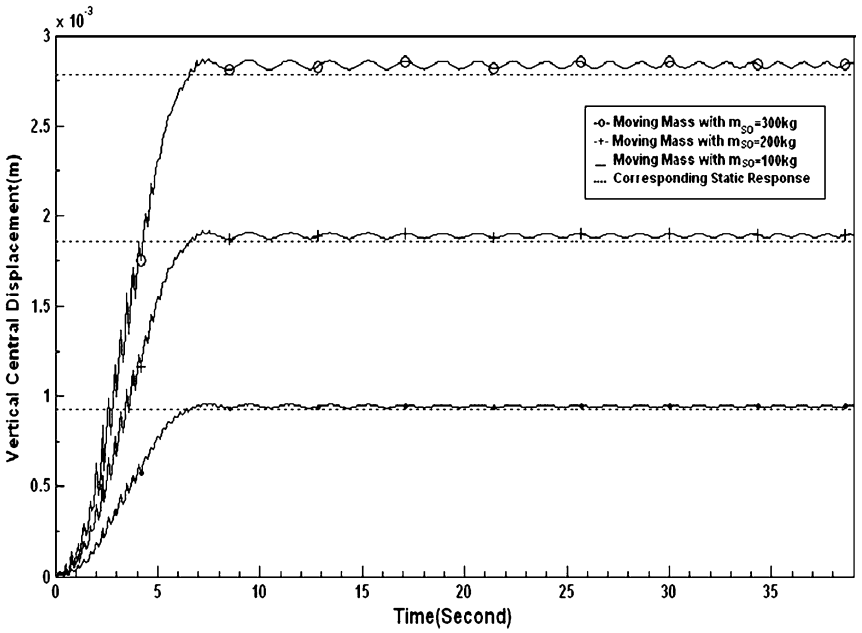

Fig. 12. The influence of the mass of the swinging object on the vertical displacements of central point C_P.

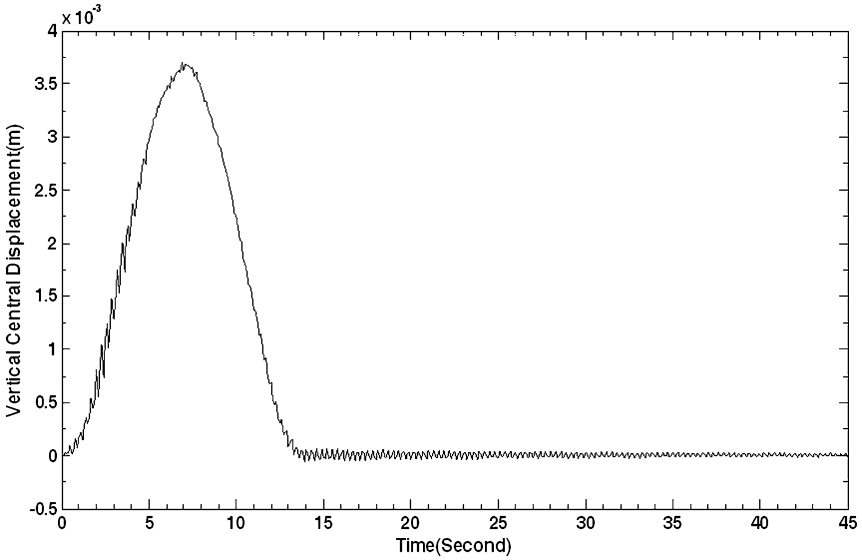

Fig. 13. Time history for vertical central vibration of the top beam with mass $m_{SO} = 400\ kg$ and the moving trolley speed $\mathrm{V}_{\mathrm{T}}^{1}(\mathrm{t})$.

4.3. Influence of moving trolley hoisting a swinging object on a mobile three-dimensional portal frame

In this section, the dynamic response of a three-dimensional framework shown in Fig. 1 due to a moving trolley hoisting a swinging object is studied. The trolley moves with the speed of V_T described in table 1 and the Gantry crane moves in the y direction with velocity history of $\mathrm{V_{GC}(t)}$ defined in Table 2.

Figure 16 illustrates the influence of the speed of the trolley on **φ(t)**. This figure shows both linear and nonlinear responses of **φ(t)** of hoisted object. The mass of the swinging object is

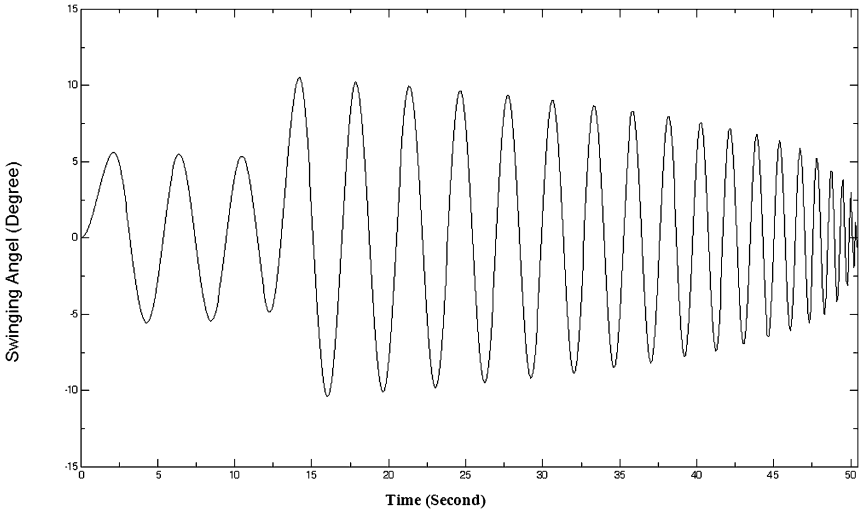

Fig. 14. Time history of the swinging angle $\theta(t)$.

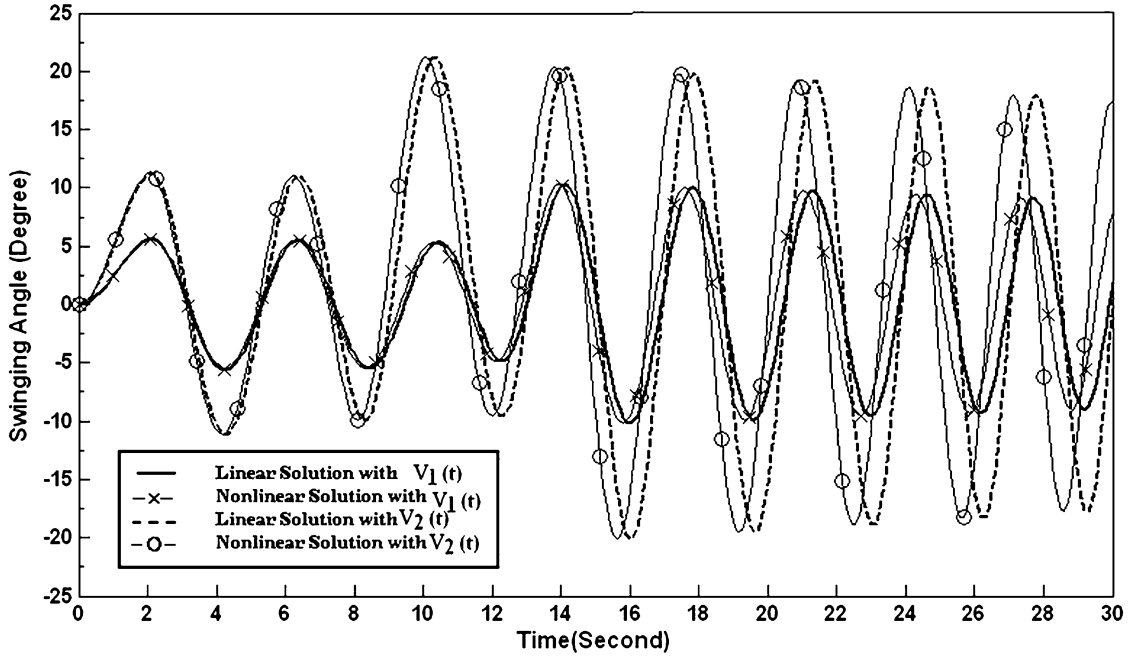

Fig. 15. Influence of the speed of the trolley on the angle of swinging object in x-y plane (i.e. $\theta(t)$) due to linear and nonlinear solution.

$m_{SO}=400$ kg. From this figure, it is seen that the difference between the linear and nonlinear solution increases as the time passes. Moreover, the difference between linear and nonlinear solution increases with the increase of swinging angle $\boldsymbol{\varphi(t)}$.

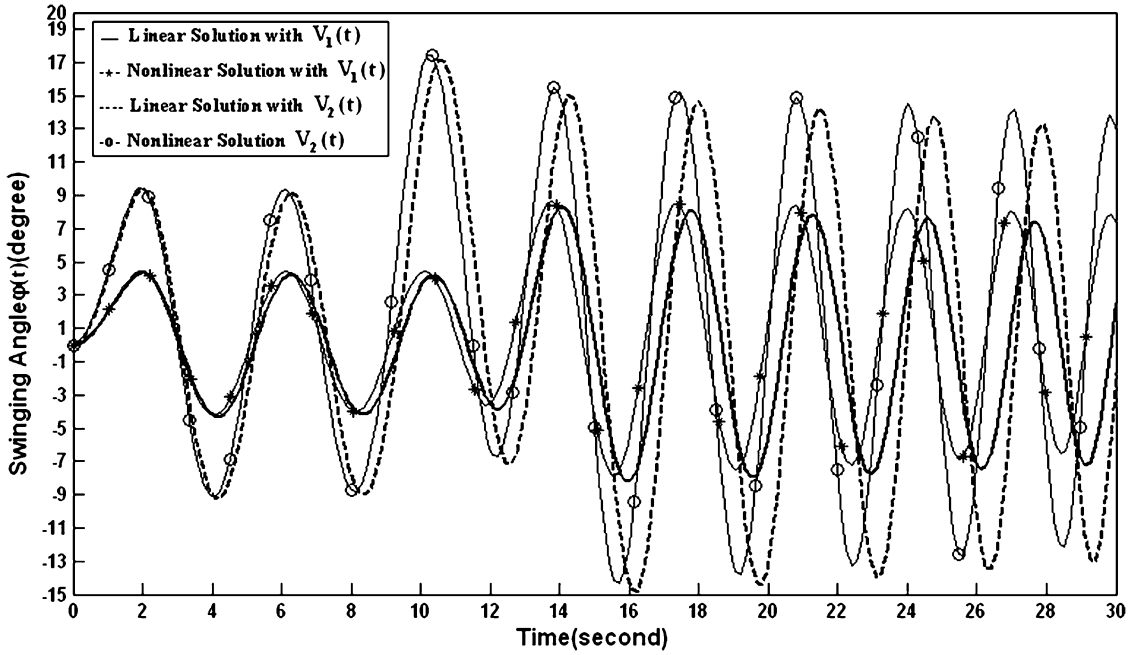

Fig. 16. Influence of the speed of the trolley on the angle between swinging object and x– y plane (i.e. $\boldsymbol{\varphi(t)}$) due to linear and nonlinear solution.

Figure 17 shows the influence of the magnitude of the mass of the swinging object on the displacements of the central point C_P in the $\bar{z}$ direction, where the velocity history of the trolley is $V_T{}^2(t)$. In this figure, it is seen that the amplitude of nonlinear solution is greater than the amplitude of linear solution. This may be because of greater amplitude of swinging angle of nonlinear solution than linear solution as shown in Fig. 16. Also, as one may see the difference between the linear and nonlinear solution increases as the time passes.

Figure 18 shows the influence of the moving speed of the trolley on the displacements of the central point C_P in the $\bar{\mathbf{x}}$ direction ($\bar{x}_C$), while the mass of the swinging object is $m_{SO} = 400$ kg and the velocity history of the framework is $V_{GC}(t)$. It is seen that with the increase of acceleration and velocity of the trolley, the axial central displacement increases. It is also worth noting that the swinging angle of the hoisted object has significant influence on the vertical and axial responses of the top beam for large swinging angle ($\theta(t) > 6^\circ$).

5. CONCLUSIONS

A combinational (Runge-kutta-Newmark) solution technique was used to solve nonlinear set of equations of motion of a three dimensional gantry crane hoisting a swinging object. A computer code was provided to obtain the time-variant external nodal force on the whole structure. The technique was implemented for three different structures: I) Two-dimensional gantry crane subjected to a moving mass, II) Two-dimensional gantry crane subjected to moving trolley hoisting a swinging object, III) Three-dimensional mobile gantry crane subjected to moving trolley hoisting a swinging object. Important points of the simulated results have been summarized as follow:

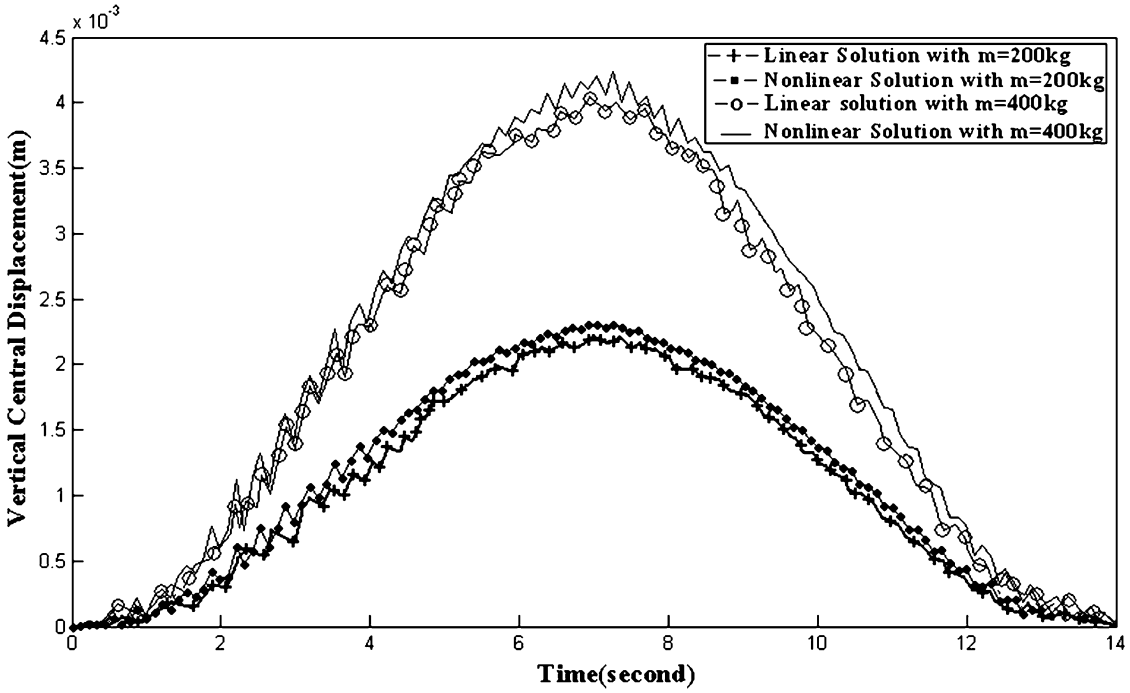

Fig. 17. Influence of the magnitude of the mass of the swinging object on the displacements of the central point C_P in $\bar{z}$ direction.

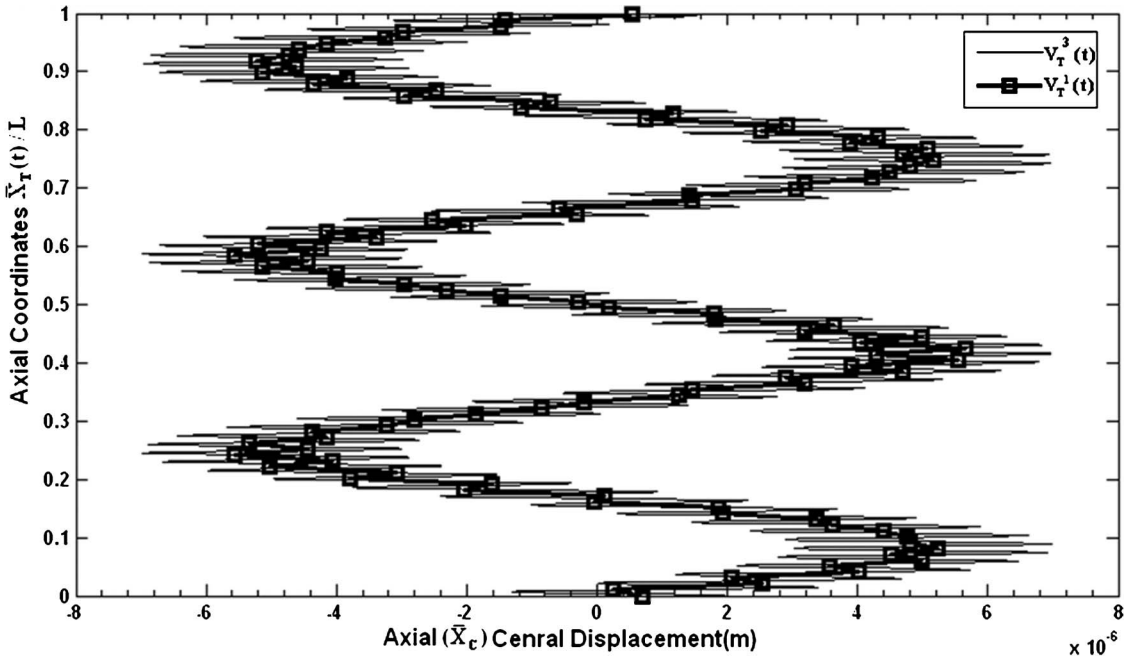

Fig. 18. Influence of the moving speed of the trolley on displacements of the central point C_P in the x direction ($\bar{x}_C$).

1. Increasing the speed and acceleration of the trolley does not influence the maximum deflection of the central point C_P of the top beam, but it causes a decrease in the deflection of this point in other instants of the motion.
2. In the case of the moving trolley hoisting a swinging object (section 4.2), the dynamic response converges to a displacement which is greater than the static one. The difference between the static and the ultimate dynamic responses increases with the increase of the mass of the swinging object.
3. The vibration frequency of the swinging angle and the vertical displacement increase as the time passes because of the shortening of the cable length.
4. Speed of the trolley has a significant influence on the axial ($\bar{\mathbf{x}}_\mathbf{C}$) and vertical ($\bar{z}_C$) dynamic responses of the top beam for large swinging angles ($\theta(t) > 6^\circ$).
5. It was found that, nonlinear solutions have larger amplitudes both for the swinging angles and also the structure response. In other words, linear analysis may mislead the crane designers to smaller values of stress and deflection in comparison with the reality (nonlinear analysis).

REFERENCES

1. Fyba, L., *Vibration of solids and structures under moving loads*, Telford, London, 1999.
2. Wu, J.J., Whittaker, A.R., Cartmell, M.P., "The use of finite element techniques for calculating the dynamic response of structures to moving load," *Computers and Structures*, Vol. 78, pp. 789–799, 2000.
3. Michaltoses, G., Sophianopoulous, D. and Kounadis, A.N., "The effect of moving mass and other parameters on the dynamic response of a simply supported beam," *Journal of Sound and Vibration*, Vol. 191, pp. 357–362, 1996.

4. Lee, H., "Dynamic response of a beam with a moving mass," *Journal of Sound and Vibration*, Vol. 191, pp. 289–294, 1996.
5. Lin, Y.H. and Trethewey, M.W., "Finite element analysis of elastic beam subjected to moving dynamic loads," *Journal of Sound and Vibration*, Vol. 136, pp. 323–342, 1990.
6. Esmailzadeh, E. and Ghorashi, M., "Vibration analysis of beams traversed by uniform partially distributed moving masses," *Journal of Sound and Vibration*, Vol. 184, pp. 9–17, 1995.
7. Esmailzadeh, E. and Ghorashi, M., "Vibration analysis of a Timoshenko beam subjected to a traveling mass," *Journal of Sound Vibration*, Vol. 199, pp. 615–628, 1997.
8. Xu, X. and Xu, W. and Genin, J., "A non-linear moving mass problem," *Journal of Sound and Vibration*, Vol. 204, pp. 495, 1997.
9. Younesian, D., Kargarnovin, M.H., Thompson, D.J. and Jones, C.J.C., "Ride comfort of high-speed trains travelling over railway bridges," *Vehicle System Dynamics*, Vol. 43, No. 3, pp. 173–197, 2005.
10. Younesian, D., Kargarnovin, M.H., "Dynamics of Timoshenko beams on Pasternak foundation under moving load," *Mechanics Research Communication*, Vol. 31, No. 6, pp. 713–723, 2004.
11. Younesian, D., Kargarnovin, M.H., Thompson, D.J. and Jones, C.J.C., "Response of beams on nonlinear viscoelastic foundations to harmonic moving loads," *Computers & Structures*, Vol. 83, pp. 1865–1877, 2005.
12. Kargarnovin, M.H., Younesian, D., Thompson, D.J. and Jones, C.J.C., "Parametrically excited vibration of a Timoshenko beam on viscoealstic foundation subjected to a harmonic moving load," *Nonlinear Dynamics*, Vol. 45, pp. 75–93, 2005.
13. Ghafoori, E. and Asghari, M., "Dynamic responses of laminated composite plates traversed by a moving mass based on a first order theory," *Composite Structures*, Vol. 92, pp. 1865–1876, 2010.
14. Sorensen, K.L., Singhose, W., Dickerson, S.A., "Controller enabling precise positioning and sway reduction in bridge and gantry cranes," *Control Engineering Practice*, Vol. 15, No. 7, pp. 825–837, 2007.
15. Ghafoori, E. and Ghahremani, A.R., "Dynamic responses of a plate due to a moving oscillator using a semi-analytical method," *Journal of Vibration and Control*, In Press, 2010.
16. Singhose, W., Porter, L., Kenison, M. and Kriikku, M., "Effects of hoisting on the input shaping control of gantry cranes," *Control Engineering Practice*, Vol. 8, No. 10, pp. 1159–1165, 2000.
17. Wu, J.J., Whittaker, A.R., Cartmell, M.P., "Dynamic responses of structures to moving bodies using combined finite element and analytical methods," *Journal of Mechanical Science*, Vol. 43, pp. 2555–2379, 2001.
18. Wu, J.J., "Dynamic responses of a three-dimensional framework due to a moving carriage hoisting a swinging object," *International Journal for Numerical Methods in Engineering*, Vol. 59, pp. 1679–1702, 2004.
19. Sadeghpour, M., Yousefi, R., Ghafoori, E. and Younesian, D., "Identification of multi-degree of freedom nonlinear systems using an extended finite element method," *7th EUROMECH Solid Mechanics Conference*, Portugal, September 7–11, 2009.
20. Bathe, K.J., *Finite element Procedure in Engineering Analysis*, Prentice-Hall: Englewood Cliffs, 1982.
21. Dawe, D.J., *Matrix and Finite Element Displacement Analysis of Structures*, Oxford University Press, 1984.

APPENDIX

A. Stiffness and Mass Matrices

The elements of the space frame of the structure carry axial loading, transverse loadings, bending moments and twisting moment. The element of a rigid-jointed space frame combines the functions of the element of a planar rigid-jointed frames and the element of a grillage. Consequently the stiffness matrix of the space-frame element in its local coordinate system can be assembled very simply and directly from the corresponding stiffness matrices of the planar frame and the grillage. The stiffness matrix k for a sample beam element is given below. Eventually; the transformed stiffness matrix can be obtained with the following equation

$$\overline{k} = \tau^{t} k \tau \tag{A.1}$$

Where k is the stiffness matrix for each beam element (Eq. A.2), τ is the rotation transformation matrix and $\bar{k}$ is the transformed stiffness matrix for each beam element. It is obvious that the rotation transformation matrix,τ, is as a function of angle of the beam element respect to the global $\bar{x}\bar{y}\bar{z}$ coordinate system.

$$k = \begin{pmatrix}
\frac{AE}{l_e} & 0 & 0 & 0 & 0 & 0 & \frac{AE}{l_e} & 0 & 0 & 0 & 0 & 0 \\
0 & \frac{12EI_z}{l_e^3} & 0 & 0 & 0 & \frac{6EI_z}{l_e^2} & 0 & \frac{12EI_z}{l_e^3} & 0 & 0 & 0 & \frac{6EI_z}{l_e^2} \\
0 & 0 & \frac{12EI_y}{l_e^3} & 0 & -\frac{6EI_y}{l_e^2} & 0 & 0 & 0 & -\frac{12EI_y}{l_e^3} & 0 & -\frac{6EI_y}{l_e^2} & 0 \\
0 & 0 & 0 & \frac{GJ}{l_e} & 0 & 0 & 0 & 0 & 0 & -\frac{GJ}{l_e} & 0 & 0 \\
0 & 0 & -\frac{6EI_y}{l_e^2} & 0 & \frac{4EI_y}{l_e} & 0 & 0 & 0 & \frac{6EI_y}{l_e^2} & 0 & \frac{2EI_y}{l_e} & 0 \\
0 & \frac{6EI_z}{l_e^2} & 0 & 0 & 0 & \frac{4EI_z}{l_e} & 0 & -\frac{6EI_z}{l_e^2} & 0 & 0 & 0 & \frac{2EI_z}{l_e} \\
\frac{AE}{l_e} & 0 & 0 & 0 & 0 & 0 & \frac{AE}{l_e} & 0 & 0 & 0 & 0 & 0 \\
0 & \frac{12EI_z}{l_e^3} & 0 & 0 & 0 & -\frac{6EI_z}{l_e^2} & 0 & \frac{12EI_z}{l_e^2} & 0 & 0 & 0 & -\frac{6EI_z}{l_e^2} \\
0 & 0 & -\frac{12EI_y}{l_e^3} & 0 & \frac{6EI_y}{l_e^2} & 0 & 0 & 0 & \frac{12EI_y}{l_e^3} & 0 & \frac{6EI_y}{l_e^2} & 0 \\
0 & 0 & 0 & -\frac{GJ}{l_e} & 0 & 0 & 0 & 0 & 0 & \frac{GJ}{l_e} & 0 & 0 \\
0 & 0 & -\frac{6EI_y}{l_e^2} & 0 & \frac{2EI_y}{l_e} & 0 & 0 & 0 & \frac{6EI_y}{l_e^2} & 0 & \frac{4EI_y}{l_e} & 0 \\
0 & \frac{6EI_z}{l_e^2} & 0 & 0 & 0 & \frac{2EI_z}{l_e} & 0 & -\frac{6EI_z}{l_e^2} & 0 & 0 & 0 & \frac{4EI_z}{l_e}
\end{pmatrix} \tag{A.2}$$

The transformed mass matrix $\bar{m}$ for each element can also been obtained in the same manner. Therefore, one can do the same procedure for all elements and then assemble the stiffness and mass matrices to find the overall stiffness $\bar{K}$ and overall mass $\bar{M}$ matrices.

B. Damping Matrix

Using the theory of Rayleigh damping [20], it is straightforward to obtain the overall damping matrix from overall stiffness and mass matrices which has been determined in the last subsection

$$\left(\bar{C}\right) = \alpha(\bar{K}) + \beta(\bar{M}) \tag{B.1}$$

where α and β are constants. Orthogonality principle of the mode shapes results in

$$2\xi_i\omega_i = \alpha + \beta{\omega_i}^2 \tag{B.2}$$

Where

$$\alpha = \frac{2\omega_i\omega_j\left(\xi_i\omega_j - \xi_j\omega_i\right)}{{\omega_j}^2 - {\omega_i}^2} \tag{B.3}$$

$$\beta = \frac{2\left(\xi_j\omega_j - \xi_i\omega_i\right)}{{\omega_j}^2 - {\omega_i}^2} \tag{B.4}$$

where the damping ratio ξ_i and ξ_j correspond to any two natural frequencies of the structure, ω_i and ω_j, respectively.

C. Acceleration of the Swinging Object with Respect to the Local Coordinate System.

From Eq. (2), one may calculate the $\ddot{x}$, $\ddot{y}$ *and* $\ddot{z}$ acceleration

$$\begin{cases} \ddot{x} = \ddot{r}\cos\phi\cos\theta - \dot{r}\dot{\phi}\sin\phi\cos\theta - \dot{r}\dot{\theta}\cos\phi\sin\theta - \dot{r}\dot{\phi}\sin\phi\cos\theta \\ \quad - r\ddot{\phi}\sin\phi\cos\theta - r\dot{\phi}^2\cos\phi\cos\theta + r\dot{\phi}\dot{\theta}\sin\phi\sin\theta - \dot{r}\dot{\theta}\cos\phi\sin\theta \\ \quad + r\dot{\theta}\dot{\phi}\sin\phi\sin\theta - r\ddot{\theta}\cos\phi\sin\theta - r\dot{\theta}^2\cos\phi\cos\theta \\ \ddot{y} = \ddot{r}\cos\phi\cos\theta - \dot{r}\dot{\phi}\sin\phi\cos\theta - \dot{r}\dot{\theta}\cos\phi\sin\theta - \dot{r}\dot{\phi}\sin\phi\sin\theta \\ \quad - r\ddot{\phi}\sin\phi\sin\theta - r\dot{\phi}^2\cos\phi\sin\theta - r\dot{\phi}\dot{\theta}\sin\phi\cos\theta + \dot{r}\dot{\theta}\cos\phi\cos\theta \\ \quad - r\dot{\phi}\dot{\theta}\sin\phi\cos\theta + r\ddot{\theta}\cos\phi\cos\theta - r\dot{\theta}^2\cos\phi\sin\theta \\ \ddot{z} = \ddot{r}\sin\phi + \dot{r}\dot{\phi}\cos\phi + \dot{r}\dot{\phi}\cos\phi + r\ddot{\phi}\cos\phi - r\dot{\phi}^2\sin\phi \end{cases}$$

where $r, \dot{r}$ *and* $\ddot{r}$are respectively the magnitude of the length, velocity and acceleration of cable.